Chapter 5

Perturbation Evolution

Although heaven and earth are great, their evolution is uniform.
Although the myriad things are numerous, their governance is unitary.
–Chuang-tzu, 12

Superhorizon and subhorizon perturbation evolution take on simple asymptotic forms and interpretations under the hybrid gauge representation developed in §4.3. All component fluctuations *evolve* similarly above the horizon and assume differing forms only due to the initial conditions. We discuss the general solution to the perturbation equations valid for an arbitrary mixture of initial curvature and entropy fluctuations in a universe that passes from radiation to matter to curvature and/or cosmological constant domination. These two initial conditions distinguish the adiabatic and isocurvature growing modes. Evolution during and after horizon crossing exhibits more complicated behavior. Well under the horizon but before recombination, photon pressure in the Compton coupled photon-baryon fluid resists gravitational compression and sets up acoustic waves. In the intermediate case, gravity *drives* the acoustic oscillations. The presence of baryons and radiation feedback on the potentials alter the simple oscillatory form of the acoustic wave. These effects leave distinct signatures on CMB anisotropies in the degree to arcminute range. After recombination, the baryons are released from Compton drag and their density fluctuations can again grow by gravitational instability. The discussion here of the evolutionary properties of perturbations sets the stage for the analysis of anisotropy formation in §6 and §7.

5.1 Superhorizon Evolution

5.1.1 Total Matter Equation

Only gravity affects the evolution of the matter and radiation above the horizon scale in the total matter representation. This greatly simplifies the evolution equations since we can treat all the particle species as a combined total matter fluid without loss of information. Let us prove this assertion. Specifically, we need to show that all particle velocities are equal [84]. Ignoring particle interactions which play no role above the horizon, the Euler equations for pressureless matter and radiation components are given by

$$\dot{V}_m = -\frac{\dot{a}}{a} V_m + k\Psi, \tag{5.1}$$

$$\dot{V}_r = -\frac{\dot{a}}{a} V_T + k\Psi + \frac{1}{4} k\Delta_r, \tag{5.2}$$

where we have transformed the Newtonian Euler equation (4.43) into the total matter representation with equation (4.89). We have also neglected the small contribution from anisotropic stress.

Infall into potential wells sources the matter and radiation velocities alike. Although it attains its maximum effect near horizon crossing $k\eta \gtrsim 1$ due to causality, the fact that a given eigenmode k does not represent one physical scale alone allows infall to generate a small velocity contribution of $\mathcal{O}(k\eta)$ when $k\eta \lesssim 1$. Expansion drag on the matter causes V_m to decay as a^{-1}. However, the Euler equation for the radiation contains not only a different expansion drag term but also pressure contributions which prevent infall. Let us determine when pressure is important. The Poisson equation (4.95) requires

$$(k^2 - 3K)\Phi = \frac{3}{2}\left[\left(\frac{\dot{a}}{a}\right)^2 + K - \left(\frac{a}{a_0}\right)^2 \Omega_\Lambda H_0^2\right]\Delta_T, \tag{5.3}$$

where we have employed the Hubble equation (4.61). Since

$$\frac{\dot{a}}{a} = \begin{cases} 1/\eta & \text{RD} \\ 2/\eta, & \text{MD} \end{cases} \tag{5.4}$$

in the radiation-dominated (RD) and matter-dominated (MD) epochs, to order of magnitude

$$\Delta_T \sim (k\eta)^2 \Phi, \tag{5.5}$$

before curvature or Λ domination. Since $\Psi \simeq -\Phi$, pressure may be neglected compared with infall outside the horizon where $k\eta \ll 1$. This seemingly obvious statement is actually not true for the Newtonian gauge density perturbation since $\delta_T^N = \mathcal{O}(\Psi)$ if $k\eta \ll 1$. The appearance of the expansion drag term V_T in equation (5.2) is in fact due to the pressure contributions in the Newtonian frame. Starting from arbitrary initial conditions and in the absence of infall, the expansion will damp away velocities until $V_T = V_m = V_r = 0$. The infall source gives rise to equal velocities for all components.

We can thus describe the coupled multi-component system as a single fluid, defined by the total matter variables whose behavior does not depend on the microphysics of the components. Assuming the various species are all either fully relativistic or non-relativistic, *i.e.* employing equations (4.54) and (4.58) with their decoupled variants, we obtain

$$\dot{\Delta}_T - 3w_T\frac{\dot{a}}{a}\Delta_T = -\left(1-\frac{3K}{k^2}\right)(1+w_T)kV_T - 2\left(1-\frac{3K}{k^2}\right)\frac{\dot{a}}{a}w\Pi_T, \tag{5.6}$$

$$\dot{V}_T + \frac{\dot{a}}{a}V_T = \frac{4}{3}\frac{w_T}{(1+w_T)^2}k[\Delta_T - (1-3w_T)S] + k\Psi - \frac{2}{3}k\left(1-\frac{3K}{k^2}\right)\frac{w_T}{1+w_T}\Pi_T, \tag{5.7}$$

where we have used the entropy relation (4.50) and recall $S \equiv \Delta_m - \frac{3}{4}\Delta_r$. The difference in how V_m and V_r is damped by the expansion appears as an entropy term in the total Euler equation. Again for superhorizon scales, we can ignore the pressure term $\propto \Delta_T$ in the total Euler equation above.

The evolution of the entropy is given by the continuity equation for the number density (4.59), *i.e.* $\dot{S} = k(V_r - V_m)$, where the matter and radiation velocities are defined in a manner analogous to V_T [see equation (4.46)]. Since all components have the same velocity, S is a constant before the mode enters the horizon and, if it is present, must have been established at the initial conditions.

5.1.2 General Solution

From Radiation to Matter Domination

Before horizon crossing, radiation pressure may be neglected. Specifically this occurs at $\dot{a}/a = k$ or

$$a_H = \frac{1+\sqrt{1+8(k/k_{eq})^2}}{4(k/k_{eq})^2}, \qquad \text{RD/MD} \tag{5.8}$$

where $k_{eq} = (2\Omega_0 H_0^2 a_0)^{1/2}$ is the scale that passes the horizon at equality and $a_{eq} = 1$. Dropping the curvature and Λ contribution to the expansion and combining the total continuity

(5.6) and Euler equations (5.7) yields the second order evolution equation

$$\left\{ \frac{d^2}{da^2} - \frac{f}{a}\frac{d}{da} + \frac{1}{a^2}\left[\left(\frac{k}{k_{eq}}\right)^2 \left(1 - \frac{3K}{k^2}\right) h - g \right] \right\} \Delta_T = \left(\frac{k}{k_{eq}}\right)^2 \left(1 - \frac{3K}{k^2}\right) jS, \tag{5.9}$$

where

$$\begin{aligned} f &= \frac{3a}{4+3a} - \frac{5}{2}\frac{a}{1+a}, \\ g &= 2 + \frac{9a}{4+3a} - \frac{a}{2}\frac{6+7a}{(1+a)^2}, \\ h &= \frac{8}{3}\frac{a^2}{(4+3a)(1+a)}, \\ j &= \frac{8}{3}\frac{a}{(4+3a)(1+a)^2}. \end{aligned} \tag{5.10}$$

Here we have used $3w_T = (1+a)^{-1}$ and have dropped the anisotropic stress correction Π_T (see Appendix A.1.1). The solutions to the homogeneous equation with $S = 0$ are given by

$$\begin{aligned} U_G &= \left[a^3 + \frac{2}{9}a^2 - \frac{8}{9}a - \frac{16}{9} + \frac{16}{9}\sqrt{a+1} \right] \frac{1}{a(a+1)}, \\ U_D &= \frac{1}{a\sqrt{a+1}}, \end{aligned} \tag{5.11}$$

and represent the growing and decaying mode of adiabatic perturbations respectively. Using Green's method, the particular solution in the presence of a *constant* entropy fluctuation S becomes $\Delta_T = C_G U_G + C_D U_D + S U_I$, where U_I is given by [100]

$$U_I = \frac{4}{15}\left(\frac{k}{k_{eq}}\right)^2 \left(1 - \frac{3K}{k^2}\right) \frac{3a^2 + 22a + 24 + 4(4+3a)(1+a)^{1/2}}{(1+a)(3a+4)[1+(1+a)^{1/2}]^4} a^3. \tag{5.12}$$

From Matter to Curvature or Λ domination

After radiation becomes negligible, both the isocurvature and adiabatic modes evolve in the same manner

$$\ddot{\Delta}_T + \frac{\dot{a}}{a}\dot{\Delta}_T = 4\pi G \rho_T \left(\frac{a}{a_0}\right)^2 \Delta_T. \tag{5.13}$$

For pressureless perturbations, each mass shell evolves as a separate homogeneous universe. Since a density perturbation can be viewed as merely a different choice of the initial time surface, the evolution of the fractional shift in the scale factor $a^{-1}\delta a/\delta t$, *i.e.* the Hubble parameter H, must coincide with Δ_T. This is an example of how a clever choice of gauge simplifies the analysis. It is straightforward to check that the Friedman equations (4.61) and (4.33) do indeed imply

$$\ddot{H} + \frac{\dot{a}}{a}\dot{H} = 4\pi G\rho_T \left(\frac{a}{a_0}\right)^2 H, \tag{5.14}$$

so that one solution, the decaying mode, of equation (5.13) is $\Delta_T \propto H$ [124]. The growing mode $\Delta_T \propto D$ can easily be determined by writing its form as $D \propto HG$ and by substitution into equation (5.13)

$$\ddot{G} + \left(\frac{\dot{a}}{a} + 2\frac{\dot{H}}{H}\right)\dot{G} = 0. \tag{5.15}$$

This can be immediately solved as [124]

$$D(a) \propto H \int \frac{da}{(aH)^3}. \tag{5.16}$$

Note that we ignore pressure contributions in H. If the cosmological constant $\Lambda = 0$, this integral can be performed analytically

$$D(a) \propto 1 + \frac{3}{x} + \frac{3(1+x)^{1/2}}{x^{3/2}} \ln[(1+x)^{1/2} - x^{1/2}], \tag{5.17}$$

where $x = (\Omega_0^{-1} - 1)(a/a_0)$. In the more general case, a numerical solution to this integral must be employed. Notice that $D \propto a$ in the matter-dominated epoch and goes to a constant in the curvature or Λ-dominated epoch.

General Solution

Before curvature or Λ domination, $D \propto a$. The full solution for Δ_T, where the universe is allowed to pass through radiation, matter and curvature or Λ domination, can be simply obtained from equation (5.11) and (5.12), by replacing a with D normalized so that $D = a$ early on, *i.e.*

$$a \to D = \frac{5}{2} a_0 \Omega_0 g(a) \int \frac{da}{a} \frac{1}{g^3(a)} \left(\frac{a_0}{a}\right)^2, \tag{5.18}$$

where

$$g^2(a) = \left(\frac{a_0}{a}\right)^3 \Omega_0 + \left(\frac{a_0}{a}\right)^2 (1 - \Omega_0 - \Omega_\Lambda) + \Omega_\Lambda. \tag{5.19}$$

For convenience, we parameterize the initial amplitude of the homogeneous growing mode with the initial curvature fluctuation $\Phi(0)$. The general growing solution then becomes

$$\Delta_T = \Phi(0) U_A + S(0) U_I, \tag{5.20}$$

The evolutionary factors U_A and U_I are given by equations (5.18), (5.11), (5.12) to be

$$U_A = \frac{6}{5}\left(\frac{k}{k_{eq}}\right)^2\left(1-\frac{3K}{k^2}\right)\left[D^3+\frac{2}{9}D^2-\frac{8}{9}D-\frac{16}{9}+\frac{16}{9}\sqrt{D+1}\right]\frac{1}{D(D+1)},$$
$$U_I = \frac{4}{15}\left(\frac{k}{k_{eq}}\right)^2\left(1-\frac{3K}{k^2}\right)\frac{3D^2+22D+24+4(4+3D)(1+D)^{1/2}}{(1+D)(4+3D)[1+(1+D)^{1/2}]^4}D^3 \tag{5.21}$$

respectively. We have implicitly assumed that curvature and Λ dynamical contributions are only important well after equality $a \gg 1$. Curvature dominates over matter at $a/a_0 > \Omega_0/(1-\Omega_0-\Omega_\Lambda)$, whereas Λ dominates over matter at $a/a_0 > (\Omega_0/\Omega_\Lambda)^{1/3}$ and over curvature at $a/a_0 > [(1-\Omega_0-\Omega_\Lambda)/\Omega_\Lambda]^{1/2}$. Although we will usually only consider Λ models which are flat, these solutions are applicable to the general case.

5.1.3 Initial Conditions

Two quantities, the initial curvature perturbation and entropy fluctuation serve to entirely specify the growing solution. Adiabatic models begin with no entropy fluctuations, *i.e.* $S(0) = 0$. Isocurvature models on the other hand have no curvature perturbations initially, *i.e.* $\Phi(0) = 0$. Note that any arbitrary mixture of adiabatic and isocurvature modes is also covered by equation (5.20).

For a universe with photons, 3 families of massless neutrinos, baryons and cold collisionless matter, the entropy becomes,

$$\begin{aligned} S &= \Delta_m - \frac{3}{4}\Delta_r \\ &= (1-\frac{\Omega_b}{\Omega_0})\Delta_c + \frac{\Omega_b}{\Omega_0}\Delta_b - \frac{3}{4}(1-f_\nu)\Delta_\gamma - \frac{3}{4}f_\nu\Delta_\nu \\ &= (1-\frac{\Omega_b}{\Omega_0})[(1-f_\nu)S_{c\gamma}+f_\nu S_{c\nu}] + \frac{\Omega_b}{\Omega_0}[(1-f_\nu)S_{b\gamma}+f_\nu S_{b\nu}], \end{aligned} \tag{5.22}$$

where c represents the cold collisionless component. The neutrino fraction $f_\nu = \rho_\nu/(\rho_\nu+\rho_\gamma)$ is time independent after electron-positron annihilation, implying $f_\nu = 0.405$ for three massless neutrinos and the standard thermal history. S_{ab} is the entropy or number density fluctuation between the a and b components,

$$S_{ab} = \delta(n_a/n_b) = \frac{\Delta_a}{1+w_a} - \frac{\Delta_b}{1+w_b}. \tag{5.23}$$

Entropy conservation $\dot{S}_{ab} = 0 = \dot{S}$ then has an obvious interpretation: since the components cannot separate above the horizon, the particle number ratios must remain constant.

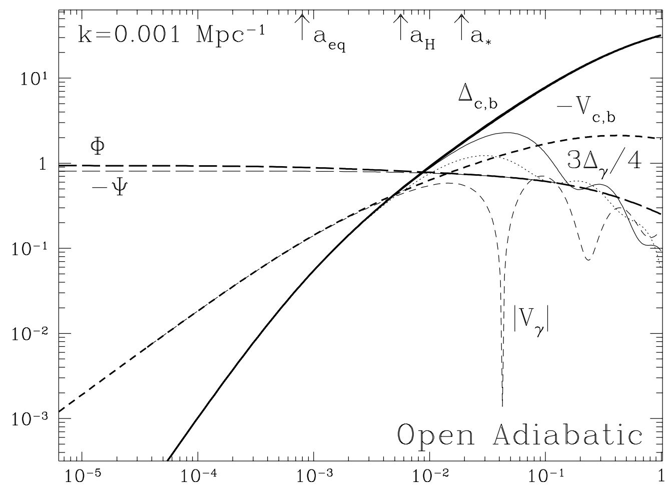

Figure 5.1: Large Scale Adiabatic Evolution

All density fluctuations evolve adiabatically $\Delta_c = \Delta_b = \frac{3}{4}\Delta_\gamma = \frac{3}{4}\Delta_\nu$ for the cold dark matter, baryons, photons and neutrinos respectively above the horizon $a < a_H$. Unlabeled dotted line is $\frac{3}{4}\Delta_\nu$. The potentials remain nearly constant until curvature domination with a 10% change at equality. The small difference between Φ and $-\Psi$ is due to the neutrino anisotropic stress (see Appendix A.1.1). After horizon crossing, the neutrinos free stream as do the photons after last scattering a_*. The model here is a fully ionized adiabatic $\Omega_0 = 0.2$, $h = 0.5$, $\Omega_b = 0.06$ universe.

The axion isocurvature model introduces density perturbations Δ_c in the cold collisionless axions in the radiation-dominated epoch without generating curvature. This implies that $S_{c\gamma} = S_{c\nu} = \Delta_c(0)$ =constant and $S_{b\gamma} = S_{b\nu} = 0$. However, the scale invariant model does not succeed in forming large scale structure and tilted models overproduce CMB anisotropies. The most promising isocurvature model is the baryon-dominated model of Peebles [125, 126] where ρ_c is assumed absent. By the same argument as above, $S_{b\gamma} = S_{b\nu} = \Delta_b(0)$ initially. Of course, since there is no cold collisionless component $S_{c\gamma} = S_{c\nu} = 0$ and $S_{b\gamma} = S_{b\nu} = S$. We shall see that some versions of this model can succeed since baryon fluctuations can lead to early structure formation and reionization damping of CMB anisotropies (see §7.1.2). When displaying isocurvature models, we implicitly assume the baryonic case.

5.1.4 Component Evolution

With the definition of S [equation (5.22)], all component perturbations can be written in terms of Δ_T. The velocity and potentials are constructed as

$$\begin{aligned} V_T &= -\frac{3}{k}\frac{\dot{a}}{a}\left(1-\frac{3K}{k^2}\right)^{-1}\frac{1+a}{4+3a}\left[a\frac{d\Delta_T}{da}-\frac{1}{1+a}\Delta_T\right], \\ \Psi &= -\frac{3}{4}\left(\frac{k_{eq}}{k}\right)^2\left(1-\frac{3K}{k^2}\right)^{-1}\frac{1+a}{a^2}\Delta_T, \end{aligned} \tag{5.24}$$

where note that constant entropy assumption requires that all the velocities $V_i = V_T$. The relation for the velocity may be simplified by noting that

$$\begin{aligned} \eta &\simeq \frac{2\sqrt{2}}{k_{eq}}\left[\sqrt{1+a}-1\right] \qquad \text{RD/MD} \\ &\simeq \frac{1}{\sqrt{-K}}\cosh^{-1}\left[1+\frac{2(1-\Omega_0)}{\Omega_0}\frac{a}{a_0}\right], \qquad \text{MD/CD} \end{aligned} \tag{5.25}$$

where CD denotes curvature domination with $\Lambda = 0$. For $\Lambda \neq 0$, it must be evaluated by numerical integration. Before curvature or Λ domination

$$\frac{\dot{a}}{a} = \frac{(1+a)^{1/2}}{\sqrt{2}a}k_{eq}, \tag{5.26}$$

which can be used to explicitly evaluate (5.24).

Now let us consider the implications of the general solution (5.20). The results for the adiabatic mode are extremely simple. When the universe is dominated by radiation (RD), matter (MD), curvature (CD) or the cosmological constant (ΛD), the total density fluctuation takes the form

$$\Delta_T/\Phi(0) = \begin{cases} \frac{4}{3}(k/k_{eq})^2(1-3K/k^2)a^2 & \text{RD} \\ \frac{6}{5}(k/k_{eq})^2(1-3K/k^2)a & \text{MD} \\ \frac{6}{5}(k/k_{eq})^2(1-3K/k^2)D. & \text{CD}/\Lambda\text{D} \end{cases} \tag{5.27}$$

Moreover since $S = 0$, the components evolve together $\Delta_b = \Delta_c = \frac{3}{4}\Delta_\gamma = \frac{3}{4}\Delta_\nu$ where Δ_c is any decoupled non-relativistic component (*e.g.* CDM). The velocity and potential are given by

$$V_T/\Phi(0) = \begin{cases} -\frac{\sqrt{2}}{2}(k/k_{eq})a & \text{RD} \\ -\frac{3\sqrt{2}}{5}(k/k_{eq})a^{1/2} & \text{MD} \\ -\frac{6}{5}(k/k_{eq})\dot{D}/k_{eq}, & \text{CD}/\Lambda\text{D} \end{cases} \tag{5.28}$$

$$\Psi/\Phi(0) = -\Phi/\Phi(0) = \begin{cases} -1 & \text{RD} \\ -\frac{9}{10} & \text{MD} \\ -\frac{9}{10}D/a. & \text{CD}/\Lambda\text{D} \end{cases} \tag{5.29}$$

An example of the evolution is plotted in Fig. 5.1.

We can also generate the Newtonian temperature perturbation from the gauge transformation

$$\Theta_0 = \frac{\Delta_\gamma}{4} - \frac{\dot a}{a}\frac{V_T}{k}, \tag{5.30}$$

which yields

$$\Theta_0/\Phi(0) = \begin{cases} \frac{1}{2} & \text{RD} \\ \frac{3}{5} & \text{MD} \\ \frac{3}{2} - \frac{9}{10}D/a. & \text{CD}/\Lambda\text{D} \end{cases} \tag{5.31}$$

In fact, these relations are far easier to derive in the Newtonian gauge itself where $\dot\Theta_0 = \dot\Phi$. Note that in the matter-dominated epoch, $\Theta_0 = -\frac{2}{3}\Psi$ which will be important for the Sachs-Wolfe effect (see §6.2).

Contrast this with the isocurvature evolution,

$$\Delta_T/S(0) = \begin{cases} \frac{1}{6}\,(k/k_{eq})^2(1-3K/k^2)a^3 & \text{RD} \\ \frac{4}{15}(k/k_{eq})^2(1-3K/k^2)a & \text{MD} \\ \frac{4}{15}(k/k_{eq})^2(1-3K/k^2)D. & \text{CD}/\Lambda\text{D} \end{cases} \tag{5.32}$$

In baryonic models

$$\Delta_b = \frac{1}{4+3a}[4S + 3(1+a)\Delta_T], \tag{5.33}$$

and

$$\begin{aligned} \Delta_\nu &= \frac{4}{3}(\Delta_b - S_{b\nu}), \\ \Delta_\gamma &= \frac{4}{3}(\Delta_b - S_{b\gamma}). \end{aligned} \tag{5.34}$$

Recall that since the curvature perturbation vanishes initially $S_{b\nu} = S_{b\gamma} = S$. From these relations, we obtain

$$\Delta_b/S(0) = \begin{cases} 1 - \frac{3}{4}a & \text{RD} \\ \frac{4}{3}\left[a^{-1} + \frac{1}{5}(k/k_{eq})^2(1-3K/k^2)a\right] & \text{MD} \\ \frac{4}{3}\left[a^{-1} + \frac{1}{5}(k/k_{eq})^2(1-3K/k^2)D\right], & \text{CD}/\Lambda\text{D} \end{cases} \tag{5.35}$$

and

$$\Delta_\gamma/S(0) = \Delta_\nu/S(0) = \begin{cases} -\,a & \text{RD} \\ \frac{4}{3}\left[-1 + \frac{4}{15}(k/k_{eq})^2(1-3K/k^2)a\right] & \text{MD} \\ \frac{4}{3}\left[-1 + \frac{4}{15}(k/k_{eq})^2(1-3K/k^2)D\right], & \text{CD}/\Lambda\text{D} \end{cases} \tag{5.36}$$

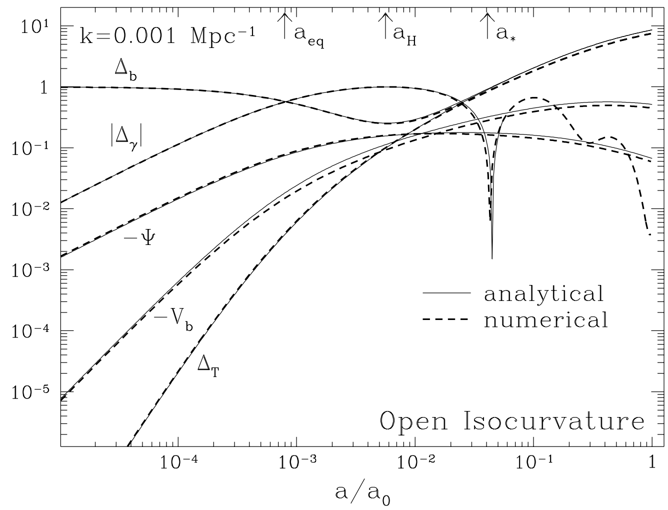

Figure 5.2: Large Scale Isocurvature Evolution

Perturbations, which originate in the baryons, are transferred to the radiation as the universe becomes more matter dominated to avoid a significant curvature perturbation. Nonetheless, radiation fluctuations create total density fluctuations from feedback. These adiabatic fluctuations in Δ_T dominate over the original entropy perturbation near horizon crossing a_H in the matter dominated epoch. The single fluid approximation cannot extend after last scattering for the photons a_*, since free streaming will damp Δ_γ away. After curvature domination, the total density is prevented from growing and thus leads to decay in the gravitational potential Ψ.

for the baryon and radiation components. Lastly, the velocity, potential, and photon temperature also have simple asymptotic forms,

$$V_T/S(0) = \begin{cases} -\frac{\sqrt{2}}{8}(k/k_{eq})a^2 & \text{RD} \\ -\frac{2\sqrt{2}}{15}(k/k_{eq})a^{1/2} & \text{MD} \\ -\frac{4}{15}(k/k_{eq})\dot{D}/k_{eq}, & \text{CD}/\Lambda\text{D} \end{cases} \tag{5.37}$$

$$\Psi/S(0) = -\Phi/S(0) = \begin{cases} -\frac{1}{8}a & \text{RD} \\ -\frac{1}{5} & \text{MD} \\ -\frac{1}{5}D/a, & \text{CD}/\Lambda\text{D} \end{cases} \tag{5.38}$$

$$\Theta_0/S(0) = \begin{cases} -\frac{1}{8}a & \text{RD} \\ -\frac{1}{5} & \text{MD} \\ -\frac{1}{5}D/a. & \text{CD}/\Lambda\text{D} \end{cases} \tag{5.39}$$

The equality of Θ and Ψ is easy to understand in the Newtonian gauge where $\dot{\Theta}_0 = -\dot{\Phi}$. In Fig. 5.2, we display an example of the isocurvature component evolution.

5.1.5 Discussion

Let us try to interpret these results physically. The isocurvature condition is satisfied by initially placing the fluctuations in the baryons $\Delta_b = S(0)$ with $\Delta_\gamma = 0$, so that $\Delta_T = 0$. As the universe evolves however, the relative significance of the baryon fluctuation $\Delta_b \rho_b / \rho_T$ for the total density fluctuation Δ_T grows as a. To compensate, the photon and neutrino fluctuations grow to be equal and opposite $\Delta_\gamma = \Delta_\nu = -aS(0)$. The tight-coupling condition $\dot{\Delta}_b = \frac{3}{4}\dot{\Delta}_\gamma$ implies then that the baryon fluctuation must also decrease so that $\Delta_b = (1 - 3a/4)S(0)$. The presence of Δ_γ means that there is a gradient in the photon energy density. This gradient gives rise to a dipole V_γ as the regions come into causal contact [see equation (4.54)], *i.e.* $V_\gamma \propto k\eta\Delta_\gamma \propto -ka^2 S(0)$. The same argument holds for the neutrinos. Constant entropy requires that the total fluid move with the photons and neutrinos $V_T = V_\gamma$, and thus infall, produced by the gradient in the velocity, yields a total density perturbation $\Delta_T \propto -k\eta(1 - 3K/k^2)V_T \propto k^2(1 - 3K/k^2)a^3 S(0)$ [see equation (5.6)]. This is one way of interpreting equation (5.21) and the fact that the entropy provides a source of total density fluctuations in the radiation-dominated epoch [73]

A similar analysis applies for adiabatic fluctuations, which begin instead with finite potential Ψ. Infall implies $V_T \propto k\eta\Psi(0) \simeq -k\eta\Phi(0)$, which then yields $\Delta_T \propto -k\eta V_T \propto k^2(1 - 3K/k^2)a^2\Phi(0)$, thereby also keeping the potential constant. Compared to the adiabatic case, the isocurvature scenario predicts total density perturbations which are smaller by one factor of a in the radiation-dominated epoch as might be expected from cancellation.

After radiation domination, both modes grow in pressureless linear theory $\Delta_T \propto D$ [*c.f.* equations (5.27) and (5.32)]. Whereas in the radiation-dominated limit, the entropy term S and the gravitational infall term Ψ are comparable in equation (5.6), the entropy source is thereafter suppressed by $w_T = p_T/\rho_T$, making the isocurvature and adiabatic evolutions identical. Furthermore, since the growth of Δ_T is suppressed in open and Λ-dominated universes, the potential Ψ decays which has interesting consequences for anisotropies as we shall see in §6.2.

5.2 Subhorizon Evolution before Recombination

As the perturbation enters the horizon, we can no longer view the system as a single fluid. Decoupled components such as the neutrinos free stream and change the number density, *i.e.* entropy, fluctuation. However, above the photon diffusion scale, the photons and baryons are still tightly coupled by Compton scattering until recombination. Since even then the diffusion length is much smaller than the horizon η_*, it is appropriate to combine the photon and baryon fluids for study [92, 147]. In this section, we show that photon pressure resists the gravitational compression of the photon-baryon fluid, leading to *driven* acoustic oscillations [82] which are then damped by photon diffusion.

5.2.1 Analytic Acoustic Solutions

At intermediate scales, neither radiation pressure nor gravity can be ignored. Fortunately, their effects can be analytically separated and analyzed [82]. Since photon-baryon tight coupling still holds, it is appropriate to expand the Boltzmann equation (4.54) and the Euler equation (4.58) for the baryons in the Compton scattering time $\dot{\tau}^{-1}$ [127]. To zeroth order, we regain the tight-coupling identities,

$$\begin{aligned} \dot{\Delta}_\gamma &= \frac{4}{3}\dot{\Delta}_b, \qquad (\text{or } \dot{\Theta}_0 = \frac{1}{3}\dot{\delta}_b^N) \\ \Theta_1 &\equiv V_\gamma = V_b, \\ \Theta_\ell &= 0. \qquad \ell \geq 2 \end{aligned} \tag{5.40}$$

These equations merely express the fact that the radiation is isotropic in the baryon rest frame and the density fluctuations in the photons grow adiabatically with the baryons. Substituting the zeroth order solutions back into equations (4.54) and (4.58), we obtain the iterative first order solution,

$$\begin{aligned} \dot{\Theta}_0 &= -\frac{k}{3}\Theta_1 - \dot{\Phi}, \\ \dot{\Theta}_1 &= -\frac{\dot{R}}{1+R}\Theta_1 + \frac{1}{1+R}k\Theta_0 + k\Psi, \end{aligned} \tag{5.41}$$

where we have used the relation $\dot{R} = (\dot{a}/a)R$. The tight-coupling approximation eliminates the multiple time scales and the infinite hierarchy of coupled equations of the full problem. In fact, this simple set of equations can readily be solved numerically [147]. To solve them analytically, let us rewrite it as a single second order equation,

$$\ddot{\Theta}_0 + \frac{\dot{R}}{1+R}\dot{\Theta}_0 + k^2 c_s^2 \Theta_0 = F, \tag{5.42}$$

where the photon-baryon sound speed is

$$c_s^2 \equiv \frac{\dot{p}_\gamma}{\dot{\rho}_\gamma + \dot{\rho}_b} = \frac{1}{3}\frac{1}{1+R}, \tag{5.43}$$

assuming $p_b \simeq 0$ and

$$F = -\ddot{\Phi} - \frac{\dot{R}}{1+R}\dot{\Phi} - \frac{k^2}{3}\Psi, \tag{5.44}$$

is the forcing function. Here $\ddot{\Phi}$ represents the dilation effect, $\dot{\Phi}$ the modification to expansion damping, and Ψ the gravitational infall. The homogeneous $F = 0$ equation yields the two fundamental solutions under the adiabatic approximation,

$$\begin{aligned} \theta_a &= (1+R)^{-1/4}\cos kr_s, \\ \theta_b &= (1+R)^{-1/4}\sin kr_s, \end{aligned} \tag{5.45}$$

where the sound horizon is

$$r_s = \int_0^\eta c_s d\eta' = \frac{2}{3}\frac{1}{k_{eq}}\sqrt{\frac{6}{R_{eq}}}\ln\frac{\sqrt{1+R}+\sqrt{R+R_{eq}}}{1+\sqrt{R_{eq}}}. \tag{5.46}$$

The phase relation $\phi = kr_s$ just reflects the nature of acoustic oscillations. If the sound speed were constant, it would yield the expected dispersion relation $\omega = kc_s$.

The adiabatic or WKB approximation assumes that the time scale for the variation in the sound speed is much longer than the period of the oscillation. More specifically, the mixed $\dot{R}\dot{\Theta}_0$ is included in this first order treatment, but second order terms are dropped under the assumption that

$$(kc_s)^2 \gg (1+R)^{1/4}\frac{d^2}{d\eta^2}(1+R)^{-1/4}, \tag{5.47}$$

or

$$\begin{aligned} (kc_s)^2 &\gg \frac{\dot{R}^2}{(1+R)^2} \\ &\gg \frac{\ddot{R}}{1+R}. \end{aligned} \tag{5.48}$$

It is therefore satisfied at early times and on small scales. Even at last scattering the approximation holds well for $k > 0.08h^3$ Mpc^{-1} if $R < 1$ and $a > 1$, as is the case for the standard CDM model.

Now we need to take into account the forcing function $F(\eta)$ due to the gravitational potentials Ψ and Φ. Employing the Green's method, we construct the particular solution,

$$\hat{\Theta}_0(\eta) = C_1\theta_a(\eta) + C_2\theta_b(\eta) + \int_0^\eta \frac{\theta_a(\eta')\theta_b(\eta) - \theta_a(\eta)\theta_b(\eta')}{\theta_a(\eta')\dot{\theta}_b(\eta') - \dot{\theta}_a(\eta')\theta_b(\eta')}F(\eta')d\eta'. \tag{5.49}$$

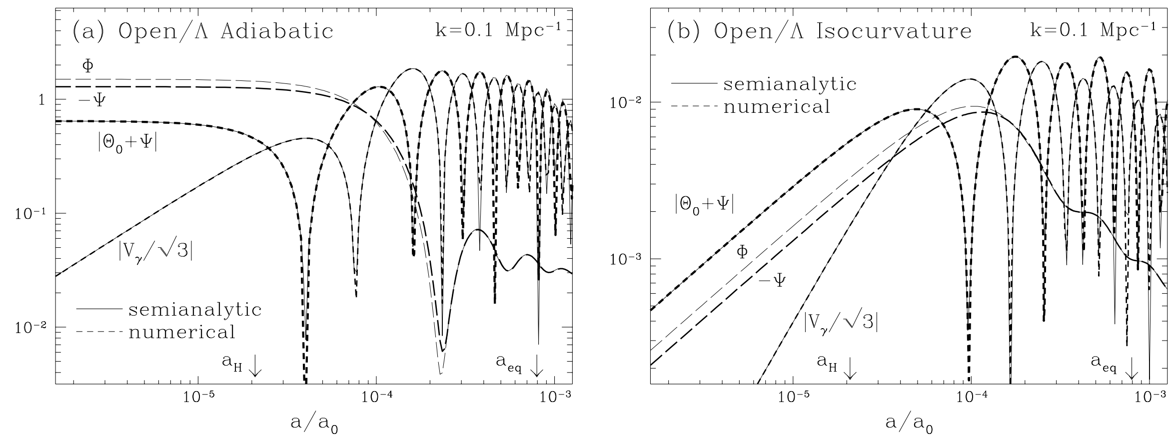

Figure 5.3: Acoustic Oscillations

Pressure resists the gravitational forces of compressional (adiabatic) and rarefaction (isocurvature) leading to acoustic oscillations. Baryons increase the gravitating mass leading to higher compressional peaks, which dominate over the rarefaction peaks and the Doppler line of sight velocity contribution $V_\gamma/\sqrt{3}$ as R is increased. Whereas the isocurvature case has $\Omega_0 = \Omega_b$, the adiabatic model has $\Omega_b = 0.06$ and a consequently smaller R. Also displayed here is the semianalytic approximation described in the text, which is essentially exact. The small difference in the numerical amplitudes of Φ and Ψ is due to the anisotropic stress of the neutrinos (see §A.1.1). Here $\Omega_0 = 0.2$ and $h = 0.5$.

Equation (5.45) implies

$$\theta_a(\eta')\theta_b(\eta) - \theta_a(\eta)\theta_b(\eta') = [1+R(\eta)]^{-1/4}[1+R(\eta')]^{-1/4}\sin[kr_s(\eta) - kr_s(\eta')]\,, \tag{5.50}$$

and

$$\theta_a(\eta')\dot\theta_b(\eta') - \dot\theta_a(\eta')\theta_b(\eta') = \frac{k}{\sqrt{3}}[1+R(\eta')]^{-1}\,. \tag{5.51}$$

With C_1 and C_2 fixed by the initial conditions, the solution in the presence of the source F then becomes [82]

$$\begin{aligned}[1+R(\eta)]^{1/4}\hat\Theta_0(\eta) \;=\; & \Theta_0(0)\cos kr_s(\eta) + \frac{\sqrt{3}}{k}[\dot\Theta_0(0) + \frac{1}{4}\dot R(0)\Theta_0(0)]\sin kr_s(\eta) \\ & + \frac{\sqrt{3}}{k}\int_0^\eta d\eta'[1+R(\eta')]^{3/4}\sin[kr_s(\eta) - kr_s(\eta')]F(\eta')\,,\end{aligned} \tag{5.52}$$

and $k\Theta_1 = -3(\dot\Theta_0 + \dot\Phi)$. The potentials in F can be approximated from their large (§5.1.4) and small (§5.2.3) scale solutions. As we shall show in Appendix A.2.2, this can lead to extremely accurate solutions. To show the true power of this technique here, we instead employ their numerical values in Fig. 5.3. The excellent agreement with the full solution indicates that our technique is limited only by our knowledge of the potentials.

5.2.2 Driven Acoustic Oscillations

Baryon Drag

Some basic features of the acoustic oscillations are worthwhile to note. Let us start with a toy model in which the potential is constant $\dot{\Psi} = 0 = \dot{\Phi}$. This corresponds to a universe which was always matter dominated. Let us also assume that the baryon-photon ratio R is constant. Of course neither of these assumptions are valid for the real universe, but as we shall see the generalization to realistic cases is qualitatively simple. Under these assumption, the solution of equation (5.42) is obvious,

$$\hat{\Theta}_0(\eta) = [\Theta_0(0) + (1+R)\Psi]\cos(kr_s) + \frac{1}{kc_s}\dot{\Theta}_0(0)\sin(kr_s) - (1+R)\Psi, \tag{5.53}$$

where the sound horizon reduces to $r_s = c_s\eta$. Several basic features are worth noting:

1. The zero point of the oscillation $\Theta_0 = -(1+R)\Psi$ is increasingly shifted with the baryon content.
2. The amplitude of the oscillation increases with the baryon content R.
3. The redshift Ψ from climbing out of potential wells cancels the $R = 0$ zero point shift.
4. Adiabatic initial conditions where $\Theta_0(0) =$ constant and isocurvature initial conditions where $\dot{\Theta}_0(0) =$ constant stimulate the cosine and sine harmonic respectively.

Of course here $\dot{\Theta}_0(0)$ does not really describe the isocurvature case since here $\Phi \neq 0$ in the initial conditions. We will see in the next section what difference this makes.

The zero point of the oscillation is the state at which the forces of gravity and pressure are in balance. If the photons dominate, $R \to 0$ and this balance occurs at $\Theta_0 = -\Psi$ reflecting the fact that in equilibrium, the photons are compressed and hotter inside the potential well. Infall not only increases the number density of photons but also their energy through gravitational blueshifts. It is evident however that when the photons climb back out of the well, they suffer an equal and opposite effect. Thus the effective temperature is $\Theta_0 + \Psi$. It is this quantity that oscillates around zero if the baryons can be neglected.

Baryons add gravitational and inertial mass to the fluid without raising the pressure. We can rewrite the oscillator equation (5.42) as

$$(1+R)\ddot{\Theta}_0 + \frac{k^2}{3}\Theta_0 = -(1+R)\frac{k^2}{3}\Psi, \tag{5.54}$$

neglecting changes in R and Φ. Note that $m_{\rm eff} = 1 + R$ represents the effective mass of the oscillator. Baryonic infall drags the photons into potential wells and consequently leads to greater compression shifting the effective temperature to $-R\Psi$. All compressional phases will be enhanced over rarefaction phases. This explains the alternating series of peak amplitudes in Fig. 5.3b where the ratio R is significant at late times. In the lower R case of Fig. 5.3a, the effect is less apparent. Furthermore, a shift in the zero point implies larger amplitude oscillations since the initial displacement from the zero point becomes larger.

Adiabatic and isocurvature conditions also have different phase relations. Peak fluctuations occur for $kr_s = m\pi$ and $kr_s = (m - 1/2)\pi$ for adiabatic and isocurvature modes respectively. Unlike their adiabatic counterpart, isocurvature conditions are set up to resist gravitational attraction. Thus the compression phase is reached for odd m adiabatic peaks and even m isocurvature peaks.

Doppler Effect

The bulk velocity of the fluid along the line of sight $V_\gamma/\sqrt{3}$ causes the observed temperature to be Doppler shifted. From the continuity equation (5.41), the acoustic velocity becomes

$$\frac{V_\gamma(\eta)}{\sqrt{3}} = \frac{\sqrt{3}}{k}\dot{\Theta}_0 = \sqrt{3}[\Theta_0(0) + (1+R)\Psi]c_s\sin(kr_s) + \frac{\sqrt{3}}{k}\dot{\Theta}_0(0)\cos(kr_s), \tag{5.55}$$

assuming $\dot{\Phi} = 0$, which yields the following interesting facts:

1. The velocity is $\pi/2$ out of phase with the temperature.
2. The zero point of the oscillation is not displaced.
3. The amplitude of the oscillation is reduced by a factor of $\sqrt{3}c_s = (1+R)^{-1/2}$ compared with the temperature.

Because of its phase relation, the velocity contribution will fill in the zeros of the temperature oscillation. Velocity oscillations, unlike their temperature counterparts are symmetric around zero. The *relative* amplitude of the velocity compared with the temperature oscillations also decreases with the baryon content R. For the same initial displacement, conservation of energy requires a smaller velocity as the mass increases. Together the zero point shift and the increased amplitude of temperature perturbations is sufficient to make compressional temperature peaks significantly more prominent than velocity or rarefaction peaks (see Fig. 5.3b).

Effective Mass Evolution

In the real universe however, R must grow from zero at the initial conditions and adiabatically changes the effective mass of the oscillator $m_{\rm eff} = (1 + R)$. While the statements above for constant R are qualitatively correct, they overestimate the effect. The exact solution given in equation (5.52) must be used for quantitative work.

Notice that the full first order relation (5.41) is exactly an oscillator with time-varying mass:

$$\frac{d}{d\eta}(1+R)\dot{\Theta}_0 + \frac{k^2}{3}\Theta_0 = -(1+R)\frac{k^2}{3}\Psi - \frac{d}{d\eta}(1+R)\dot{\Phi}, \tag{5.56}$$

where the last term on the rhs is the dilation effect from $\dot{\Theta}_0 = -\dot{\Phi}$. This form exposes a new feature due to a time varying effective mass. Treating the effective mass as an oscillator parameter, we can solve the homogeneous part of equation (5.56) under the adiabatic approximation. In classical mechanics, the ratio of the energy $E = \frac{1}{2}m_{\rm eff}\omega^2 A^2$ to the frequency ω of an oscillator is an adiabatic invariant. Thus the amplitude scales as $A \propto \omega^{1/2} \propto (1+R)^{-1/4}$, which explains the appearance of this factor in equation (5.45).

Driving Force and Radiation Feedback

Now let us consider a time varying potential. In any situation where the matter does not fully describe the dynamics, feedback from the radiation into the potential through the Poisson equation can cause time variation. For isocurvature conditions, we have seen that radiation feedback causes potentials to grow from zero outside the horizon (see §5.1 and Fig. 5.2). The net effect for the isocurvature mode is that outside the sound horizon, fluctuations behave as $\Theta = -\Phi \simeq \Psi$ [see equation (5.39)]. After sound horizon crossing, radiation density perturbations cease to grow, leading to a decay in the gravitational potential in the radiation-dominated epoch. Thus scales that cross during matter domination experience more growth and are enhanced over their small scale counterparts. Furthermore, morphologically $-\ddot{\Phi} - k^2\Psi/3 \propto \sin(kr_s)$ leading to near resonant driving of the sine mode of the oscillation until sound horizon crossing. This supports our claim above that $\sin(kr_s)$ represents the isocurvature mode.

The adiabatic mode exhibits contrasting behavior. Here the potential is constant outside the sound horizon and then decays like the isocurvature case. However, it is the decay itself that drives the oscillation since the form of the forcing function becomes approximately $-\ddot{\Phi} - k^2\Psi/3 \propto \cos(kc_s)$ until $kc_s\eta \sim 1$ and then dies away. In other words, the gravitational force drives the first compression without a counterbalancing effect on the subsequent rarefaction phase. Therefore, for the adiabatic mode, the oscillation amplitude is boosted at sound horizon crossing in the radiation-dominated universe which explains the prominence of the oscillations with respect to the superhorizon tail in Fig. 5.3a. One might expect from the dilation effect $\dot{\Theta} = -\dot{\Phi}$ that the temperature is boosted up to $\Theta(\eta) \simeq \Theta(0) - \Phi(\eta) + \Phi(0) \simeq \frac{3}{2}\Phi(0)$. We shall see in the next section that a more detailed analysis supports this conclusion. Therefore, unlike the isocurvature case, adiabatic modes experience an enhancement for scales smaller than the horizon at equality.

5.2.3 Damped Acoustic Oscillations

Well below the sound horizon in the radiation-dominated epoch, the gravitational potentials have decayed to insignificance and the photon-baryon fluctuations behave as simple oscillatory functions. However photon-baryon tight coupling breaks down at the photon diffusion scale. At this point, photon fluctuations are exponentially damped due to diffusive mixing and rescattering. We can account for this by expanding the Boltzmann and Euler equations for the photons and baryons respectively to second order in $\dot{\tau}^{-1}$ (see [124] and Appendix A.3.1). This gives the dispersion relation an imaginary part, making the general solution

$$\Theta_0 = C_A(1+R)^{-1/4}\mathcal{D}(\eta,k)\cos kr_s + C_I(1+R)^{-1/4}\mathcal{D}(\eta,k)\sin kr_s, \tag{5.57}$$

where C_A and C_I are constants and the damping factor is

$$\mathcal{D}(\eta,k) = e^{-(k/k_D)^2}, \tag{5.58}$$

with the damping scale

$$k_D^{-2} = \frac{1}{6}\int d\eta \frac{1}{\dot{\tau}}\frac{R^2 + 4(1+R)/5}{(1+R)^2}. \tag{5.59}$$

For small corrections to this relation due to the angular dependence of Compton scattering and polarization, see [93] and Appendix A.3.1. Since the R factors in equation (5.59) go to $\frac{4}{5}$ for $R \ll 1$ and 1 for $R \gg 1$, the damping length is approximately $\lambda_D^2 \sim k_D^{-2} \sim \int d\eta/\dot{\tau}$.

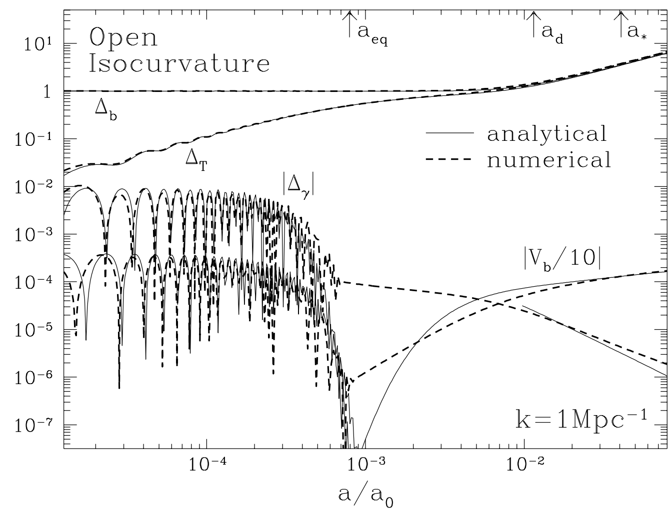

Figure 5.4: Small Scale Isocurvature Evolution

At small scales gravity may be ignored, yielding pure adiabatic oscillations. Perturbations in the photons damp once the diffusion length grows larger than the wavelength $k_D < k$. Likewise the adiabatic component of the baryon fluctuations also damps leaving them with the original entropy perturbation. After diffusion, the photons and baryons behave as separate fluids, allowing the baryons to grow once Compton drag becomes negligible $a > a_d$. Photon fluctuations are then regenerated by the Doppler effect as they diffuse across infalling baryons. The analytic approach for the photons in this limit apply between the drag epoch and last scattering $a_d < a < a_*$ (see §7.1.3). The model here is $\Omega_0 = 0.2, h = 0.5$, and no recombination.

This relation is easy to understand qualitatively. The Compton mean free path of the photons is $\lambda_C = \dot{\tau}^{-1}$. The scale on which a photon can diffuse is given by a random walk process $\sqrt{N}\lambda_C$ where the number of steps is $N = \eta/\lambda_C$. Therefore the diffusion scale is approximately $\lambda_D \simeq \sqrt{\lambda_C \eta} = \sqrt{\eta/\dot{\tau}}$.

The amplitudes of these oscillations, *i.e.* the constants C_A and C_I, are determined by the total effect of the gravitational driving force in equation (5.44). However, a simpler argument suffices for showing its general behavior. As shown in §5.1.4, isocurvature fluctuations grow like $\Delta_\gamma \simeq -aS(0)$ until sound horizon crossing. Since the sound horizon crossing is near $a_H \sim k_{eq}/k$ (see equation (5.8)), the isocurvature amplitude will be suppressed by k_{eq}/k. On the other hand, adiabatic fluctuations which grow as a^2 will have a $(k_{eq}/k)^2$ suppression factor which just cancels the factor $(k/k_{eq})^2$ from the Poisson equation [see (5.27)] when expressed in terms of the initial potential. This simple argument fixes the amplitude up to a factor of order unity.

We obtain the specific amplitude by solving equation (5.6) under the constant entropy assumption $\dot{S} = 0$. The latter approximation is not strictly valid since free streaming of the neutrinos will change the entropy fluctuation. However, since the amplitude is fixed after sound horizon crossing, which is only slightly after horizon crossing, it suffices. Under this assumption, the equation can again be solved in the small scale limit. Kodama & Sasaki [100] find that for adiabatic perturbations,

$$C_A = \frac{3}{2}\Phi(0), \quad C_I = 0, \qquad \text{(adi)} \tag{5.60}$$

from which the isocurvature solution follows via Greens method,

$$C_A = 0, \quad C_I = -\frac{\sqrt{6}}{4}\frac{k_{eq}}{k}S(0), \qquad \text{(iso)} \tag{5.61}$$

if $k \gg k_{eq}$, $k\eta \gg 1$ and $k \gg \sqrt{-K}$. As expected, the isocurvature mode stimulates the $\sin kr_s$ harmonic, as opposed to $\cos kr_s$ for the adiabatic mode.

We can also construct the evolution of density perturbations at small scales. Well inside the horizon $\Delta_\gamma = 4\Theta_0$, since total matter and Newtonian fluctuations are equivalent. The isocurvature mode solution therefore satisfies (RD/MD)

$$\Delta_\gamma / S(0) = -\sqrt{6}\left(\frac{k_{eq}}{k}\right)(1+R)^{-1/4}\mathcal{D}(a,k)\sin kr_s. \tag{5.62}$$

The tight-coupling limit implies $\dot{\Delta}_b = \frac{3}{4}\dot{\Delta}_\gamma$ which requires (RD/MD),

$$\Delta_b / S(0) = 1 - \frac{3\sqrt{6}}{4}\left(\frac{k_{eq}}{k}\right)(1+R)^{-1/4}\mathcal{D}(a,k)\sin kr_s. \tag{5.63}$$

This diffusive suppression of the adiabatic component for the baryon fluctuation is known as Silk damping [150]. After damping, the baryons are left with the original entropy perturbation S(0). Since they are surrounded by a homogeneous and isotropic sea of photons, the baryons are unaffected by further photon diffusion. From the photon or baryon continuity equations at small scales, we obtain (RD/MD)

$$V_b / S(0) = V_\gamma / C_I \simeq \frac{3\sqrt{2}}{4}\left(\frac{k_{eq}}{k}\right)(1+R)^{-3/4}\mathcal{D}(a,k)\cos kr_s. \tag{5.64}$$

As one would expect, the velocity oscillates $\pi/2$ out of phase with, and increasingly suppressed compared to, the density perturbations. Employing equations (5.62) and (5.63), we construct the total density perturbation by assuming that free streaming has damped out the neutrino contribution (RD/MD),

$$\Delta_T / S(0) = \frac{a}{1+a}\left[1 - \frac{3\sqrt{6}}{4}\frac{k_{eq}}{k}R^{-1}(1+R)^{3/4}\mathcal{D}(a,k)\sin kr_s\right]. \tag{5.65}$$

From this equation, we may derive the potential (RD/MD),

$$\Psi/S(0) = -\frac{3}{4}\left(\frac{k_{eq}}{k}\right)^2 \frac{1}{a}\left[1 - \frac{3\sqrt{6}}{4}\frac{k_{eq}}{k}R^{-1}(1+R)^{3/4}\mathcal{D}(a,k)\sin kr_s\right], \tag{5.66}$$

which decays with the expansion since Δ_T goes to a constant. In Fig. 5.4, we compare these analytic approximations with the numerical results. After damping eliminates the adiabatic oscillations, the evolution of perturbations is governed by diffusive processes. A similar analysis for adiabatic perturbations shows that diffusion damping almost completely eliminates small scale baryonic fluctuations.[1] Unlike the isocurvature case, unless CDM wells are present to reseed fluctuations, adiabatic models consequently fail to form galaxies.

5.3 Matter Evolution after Recombination

At $z_* \simeq 1000$, the CMB can no longer keep hydrogen ionized and the free electron density drops precipitously. The photons thereafter free stream until a possible epoch of reionization. The subsequent evolution of the photon fluctuations will be intensely studied in §6 and §7. Essentially, they preserve the fluctuations they possess at last scattering in the form of anisotropies. Here we will concentrate on the evolution of the matter as it is important for structure formation and feeds back into the CMB through reionization.

5.3.1 Compton Drag

Baryon fluctuations in diffusion damped scales can be regenerated after Compton scattering has become ineffective. The critical epoch is that at which the photon pressure or "Compton drag" can no longer prevent gravitational instability in the baryons. The drag on an individual baryon does not depend on the total number of baryons but rather the number of photons and its ionization state. From the baryon Euler equation (4.58) and the Poisson equation (5.24), the drag term $\propto V_b$ comes to dominate over the gravitational infall term $\propto k\Psi$ at redshifts above $z \sim 200(\Omega_0 h^2)^{1/5} x_e^{-2/5}$. Thus all modes are released from Compton drag at the same time, which we take to be

$$z_d = 160(\Omega_0 h^2)^{1/5} x_e^{-2/5}, \tag{5.67}$$

defined as the epoch when fluctuations effectively join the growing mode of pressureless linear theory.

[1]Residual fluctuations are on the order $R\Psi$ as discussed in Appendix A.3.1.

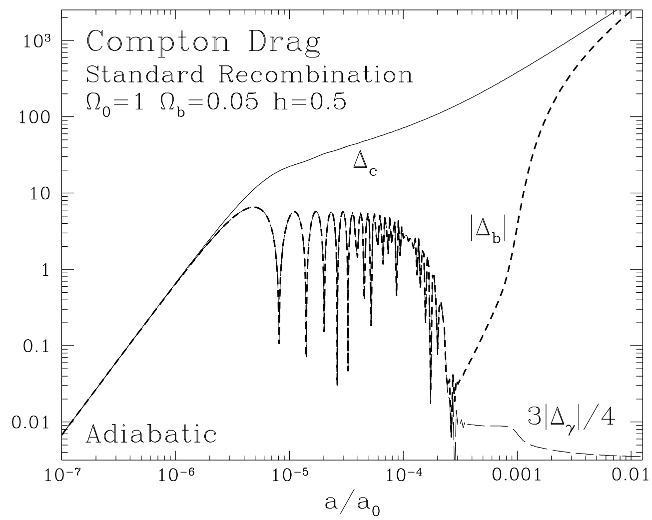

Figure 5.5: Compton Drag and Standard Recombination

After recombination, the Compton drag on the baryons decreases sharply. The residual ionization after recombination however is sufficient to slow baryon infall into dark matter wells. The baryon and cold dark matter fluctuation Δ_c only converge at $z \lesssim 100$.

It is important to realize that the drag and the last scattering redshift are generally not equal. Following the drag epoch, baryons can be treated as freely falling. If cold dark matter exists in the model, potential wells though suppressed at small scales will still exist. In adiabatic CDM models, the Silk damped baryon fluctuations under the photon diffusion scale can be regenerated as the baryons fall into the dark matter potentials (see Fig. 5.5). For isocurvature models, the entropy fluctuations remaining after Silk damping are released at rest to grow in linear theory.

One complication arises though. The collapse of baryon fluctuations after recombination can lead to small scale non-linearities. Astrophysical processes associated with compact object formation can inject enough energy to reionize the universe (see §7 and *e.g.* [58]). Ionization again couples the baryons and photons. Yet even in a reionized universe, the Compton drag epoch eventually ends due to the decreasing number density of electrons. In CDM-dominated adiabatic models, the baryons subsequently fall into the dark matter wells leaving no trace of this extra epoch of Compton coupling. The CMB also retains no memory since last scattering occurs after the drag epoch in reionized scenarios. This is not the case for baryon isocurvature models since there are no dark matter wells into which baryons might fall. Evolution in the intermediate regime therefore has a direct effect on the

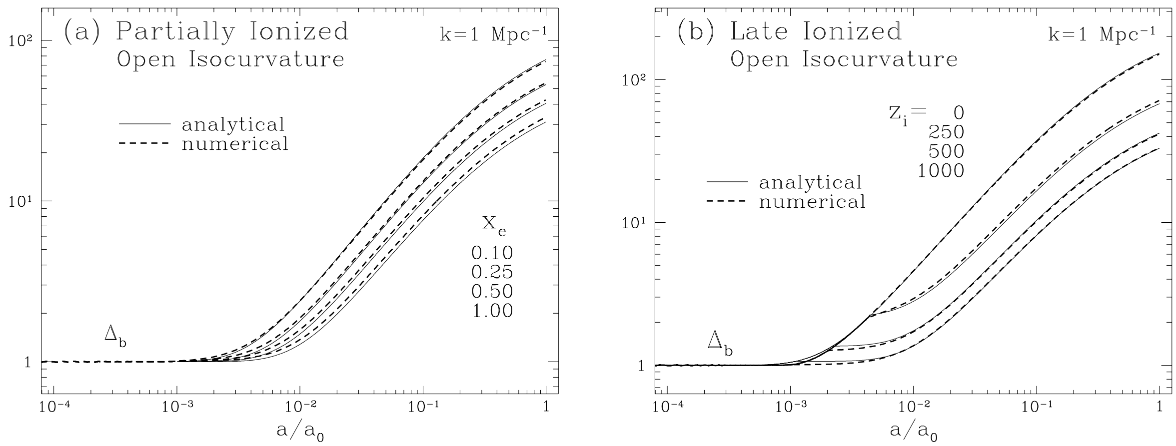

Figure 5.6: Compton Drag and Reionization

(a) The baryons are released to grow in pressureless linear theory after Compton drag becomes negligible. Raising the ionization fraction x_e delays the end of the drag epoch and makes fluctuations larger. (b) A transparent period between recombination and reionization at z_i leads to enhanced growth. After reionization, fluctuations are again suppressed until the end of the drag epoch. The model here an open baryon isocurvature one with $\Omega_0 = \Omega_b = 0.2$ $h = 0.5$.

amplitude of fluctuations in the matter and CMB today.

Reionization is also more likely in models where the initial power spectrum is tilted toward small scales. In the baryon isocurvature case, entropy fluctuations at small scales can be made quite large since they are essentially unprocessed by the pre-recombination evolution. For these reasons, we will concentrate on baryon isocurvature models in discussing Compton drag in reionized models.

5.3.2 Reionization in Isocurvature Models

Let us first consider the case where the universe was reionized immediately following standard recombination. Well before the end of the drag epoch z_d, the initial entropy fluctuations are frozen into the baryons. Well afterwards, the baryon fluctuations grow as in pressureless linear theory. An excellent empirical approximation to the behavior at intermediate times is given by

$$\Delta_b/S(0) = \mathcal{G}(a, a_d), \tag{5.68}$$

with the interpolation function

$$\mathcal{G}(a_1, a_2) = 1 + \frac{D(a_1)}{D(a_2)}\exp(-a_2/a_1), \tag{5.69}$$

where if $a_1 \gg a_2$, $\mathcal{G}(a_1, a_2) \to D(a_1)/D(a_2)$. The velocity V_T is given by the continuity equation (5.6). Notice that growth in an open and/or Λ universe is properly accounted for. This approximation is depicted in Fig. 5.6a.

Now let us consider more complicated thermal histories. Standard recombination may be followed by a significant transparent period before reionization at z_i, due to some later round of structure formation. There are two effects to consider here: fluctuation behavior in the transparent regime and after reionization. Let us begin with the first question. Near recombination, the baryons are released from drag essentially at rest and thereafter can grow in pressureless linear theory. The joining conditions then imply that $\frac{3}{5}$ of the perturbation enters the growing mode D [124], yielding present fluctuations of $\sim \frac{3}{5} C_I D(z=0)/D(z_d)$. This expression overestimates the effect for low $\Omega_0 h^2$ models due to the slower growth rate in a radiation-dominated universe. We introduce a phenomenological correction[2] by taking the effective drag epoch to be $z_d \simeq 750$ for $\Omega_0 h^2 \simeq 0.05$. The evolution is again well described by the interpolation function (5.69) so that $\Delta_b(a) = \mathcal{G}(a, a_t) C_I$. By this argument, the effective redshift to employ is $z_t \sim \frac{3}{5} z_d$.

Now let us consider the effects of reionization at z_i. After z_i, Compton drag again prevents the baryon perturbations from growing. Therefore the final perturbations will be $\Delta_b(a_0) \simeq \Delta_b(a_i) D(a_0)/D(a_d)$. Joining the transparent and ionized solutions, we obtain

$$\Delta_b/C_I = \begin{cases} \mathcal{G}(a, a_t) & a < a_g \\ \mathcal{G}(a_i, a_t)\mathcal{G}(a, a_d), & a > a_g \end{cases} \tag{5.70}$$

which is plotted in Fig. 5.6b. Since perturbations do not stop growing immediately after reionization and ionization after the drag epoch does not affect the perturbations, we take $a_g = \min(1.1 a_i, a_d)$.

For the photons, the continued ionization causes the diffusion length to grow ever larger. As the electron density decreases due to the expansion, the diffusion length reaches the horizon scale and the photons effectively last scatter. As we have seen, diffusion destroys the intrinsic fluctuations in the CMB. Any residual fluctuations below the horizon must therefore be due to the coupling with the electrons. Since last scattering follows the drag epoch, the electrons can have a significant velocity at last scattering. Thus we expect the Compton coupling to imprint a Doppler effect on the photons at last scattering. We will discuss this process in greater detail in §7.

[2] A deeper and more complete analysis of this case is given in [84].